Chalcogenide Letters Vol. 16, No. 8, August 2019, p. 417 - 423

HIGH EFFICIENCY PROCESS FOR PREPARATION OF PRISM-LIKE ANTIMONY SULPHIDES FOR APPLICATIONS: STRUCTURAL, MORPHOLOGICAL AND FORMATION MECHANISM STUDY

J. KAVINCHAN[a,*], E. SAKSORNCHAI[a], S. THONGTEM[b,c], T. THONGTEM[c,d]
[a] *School of Science, University of Phayao, Phayao 56000, Thailand*
[b]*Department of Physics and Materials Science, Faculty of Science, Chiang Mai University, Chiang Mai 50200, Thailand*
[c]*Materials Science Research Center, Faculty of Science, Chiang Mai University, Chiang Mai 50200, Thailand*
[d]*Department of Chemistry, Faculty of Science, Chiang Mai University, Chiang Mai 50200, Thailand*

Herein we present a green synthesis of prism-like antimony sulphides (Sb_2S_3) by single-step microwave assisted method which is high efficiency process with low cost and environmentally benign. The starting materials, including antimony chloride ($SbCl_3$) and thioacetamide (C_2H_5NS) dissolved in ethylene glycol under the microwave radiation at 300 W, 450 W and 600 W. The precipitates were characterized by using X-ray diffraction spectroscopy (XRD), scanning electron microscopy (SEM), energy diffraction spectroscopy (EDS), Photoluminescence (PL) spectroscopy and Raman spectroscopy illustrate the pure phase of Sb_2S_3 with prism-like morphology and well-crystalline nanostructures. In addition, the as-prepared prism-like Sb_2S_3 exhibits the optimum band gap energy that can be used as the a prospective material suitable for solar energy conversion and a possible formation mechanism was also proposed in this research.

(Received May 20, 2019; Accepted August 31, 2019)

Keywords: Green synthesis, Antimony Sulphide, X-ray diffraction spectroscopy, Photoluminescence spectroscopy, Raman spectroscopy

1. Introduction

Over a few decades, the synthesis of one-dimentinonal metal chalcogenide nanostructures such as nanorods, nanowires, nanotubes, and nanobelts has attracted considerable interest all over the world due to their superior optical, thermoelectrical and thermal properties [1-2]. To date, these binary chalcogenide materials, for instance, CdS, PbS, CdS, CuS, Sb_2S_3, *etc.* have been used as absorbing layer. Sb_2S_3 is one of the most promising materials for light harvesting candidates. In particular, it has been applied for light absorbing applications, including a solar energy conversion devices, thermoelectric devices, optoelectronic devices and photocatalysts [1-4]. Sb_2S_3 is a highly anisotropic V-VI group semiconductor with a layered structure parallel to growth direction in an orthorhombic phase [2-4]. Due to its narrow band gap, non-toxic, low cost and high adsorption coefficient ($\alpha = 10^5$ cm^{-1}) which is suitable for the absorption of visible to near infrared regions of the electromagnetic spectrum so it has been used as a potential solar absorber or absorbing layer [4].

A variety morphologies of Sb_2S_3 nanostructures have been synthesized by using various methods, for instance, chemical spray pyrolsis [2-3], hot injection method [5], chemical bath deposition [6], sonochemical method [8], simple wet chemical method [9], and microwave assisted approach [10]. However, almost methods require long reaction time. One of the most effective

---

[*] Corresponding author: jutaratkp@gmail.com

methods for synthesizing metal chalcogenide nanostructures is microwave assisted approach which has a fast heating rate and reduced time for synthesis [11-12]. Herein, we report the efficient and green synthesis of Sb_2S_3 due to this procedure has many benefits including rapid, inexpensive, simple and environmentally benign. Moreover, developing cleaner manufacturing process was also studied in this work. The results reveal that this method has high potential and reproducibility. The as-prepared products also have the clean surface with uniform of prism-like nanostructures. In addition, the phase of products and the degree of crystalline were studied by Photoluminescence spectroscopy and Raman spectroscopy. The band gap energy was determined and the possible mechanism was studied to understanding the formation process of these materials for further research.

2. Experimental

All chemical reagents used in this research were analytical grades. A typical Sb_2S_3 products were carried out by reacting of 2 mmol of $SbCl_3$ and 3 mmol of CH_3CSNH_2 (TAA) in 30.00 mL of ethylene glycol (EG) using microwave radiation at 300 W, 450 W and 600 W for 30 min. A general method to separate the precipitates was performed as follows: the precipitates were separated by filtration, washed with absolute ethanol for several times to purify products and dried at the 70 ^{O}C for 24 h for further characterization.

The phases of products were characterized by X-ray diffractometer (XRD, SIEMENS D500) operating at 20 kV, 15 mA with Kα line of a copper target. Then, the morphologies and composition of the precipitates were investigated by a scanning electron microscope (SEM, JEOL JSM-6335F) equipped with an energy dispersive X-ray (EDX) analyzer operating at 15 kV. Then, the crystallinity of products was studied by a photoluminescence (PL) spectrometer (LS 50B PerkinElmer) excited by 300 nm wavelength at room temperature and a Raman spectrometer (T64000 HORIBA Jobin Yvon) using 50 mW and 514.5 nm wavelength Ar green laser. Lastly, the optical property was also studied by a UV-visible spectrometer (Lambda 25, PerkinElmer) using a UV lamp with a resolution of 1 nm.

3. Results and discussion

The as-prepared Sb_2S_3 synthesized via single-step microwave assisted preparation of $SbCl_3$ and C_2H_5NS dissolved in ethylene glycol at 300 W, 450 W and 600 W. The crystallinity and phase of Sb_2S_3 crystalline have been indexed via an X-ray diffractometer (XRD) and the results show that the prepared products have an orthorhombic structure without impurities. Fig. 1 illustrates the XRD patterns of Sb_2S_3 synthesized in the solutions using $SbCl_3$ and C_2H_5NS as starting materials in ethylene glycol at (a) 300 W (b) 450 W (c) 600 W for 30 min. The XRD results indicated that the as-prepared Sb_2S_3 nanostructures were crystalline products that were compared to the Sb_2S_3 phase; JCPDS File no. 06-0474 [12]. According to these spectra, the as-prepared product at 600 W resulted in a well-crystallized product exhibiting more sharper reflection than the other conditions, indicating that the microwave power and temperature had effect on the crystalline degree of products, in good accordance with the provious reports [13-14].

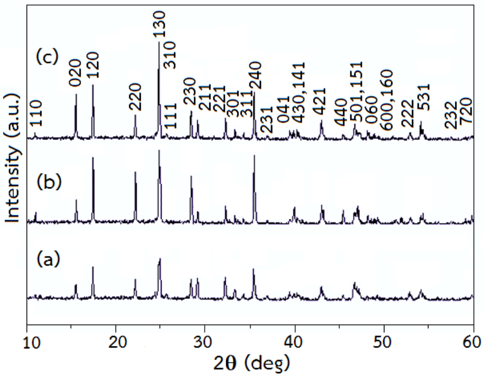

Fig. 1. XRD spectra of the as-prepared Sb_2S_3 products synthesized at (a) 300 W (b) 450 W and (c) 600 W for 30 min.

In this study, Sb_2S_3 nanostructures were produced from $SbCl_3$ and TAA in EG. The nucleation of Sb_2S_3 was associated with the formation of an orange colloidal complexes, then turned brick-red precipitaes and finally, the black precipitates were produced. In an acedic medium (pH = 2) occurs the protonation of TAA, then the intermediate product (brick red) in eq. 2 provides H_2S [14]. After that SH^- dissociates from H_2S and S^{2-} dissociates from SH^-, respectively [5, 15] (Dissociation constant; $K_1 = 5.7 \times 10^{-8}$ and $K_2 = 1.2 \times 10^{-15}$). Finally, the S^{2-} ions were released from H_2S which react with Sb^{3+} ions, which were transformed into Sb_2S_3 black precipitates [14-15]. So, the formation of Sb_2S_3 is controlled by the S^{2-} ions release rate [15]. The possible mechanism from this research was proposed from the result of this research and also proposed by the previous reports which reported by S. Srikanth *et al.* [15], O. Savaogo *et al.* [16] and K.C. Manal *et al.* [17]. The reaction equations of this reaction are describe as follows:

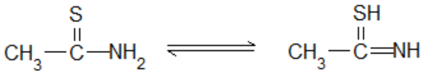

$$CH_3-\overset{\overset{S}{\|}}{C}-NH_2 \rightleftharpoons CH_3-\overset{\overset{SH}{\|}}{C}=NH \qquad (1)$$

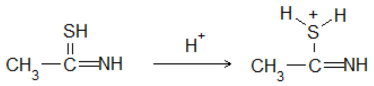

$$CH_3-\overset{\overset{SH}{\|}}{C}=NH \xrightarrow{H^+} CH_3-\overset{\overset{H\diagdown\overset{+}{S}\diagup H}{|}}{C}=NH \qquad (2)$$

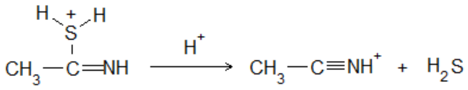

$$CH_3-\overset{\overset{H\diagdown\overset{+}{S}\diagup H}{|}}{C}=NH \xrightarrow{H^+} CH_3-C\equiv NH^+ + H_2S \qquad (3)$$

$$H_2S \longrightarrow H^+ + SH^- \qquad (4)$$

$$SH^- \longrightarrow H^+ + S^{2-} \qquad (5)$$

SEM images (Fig. 2a, 2b and 2c) show the development of Sb_2S_3 nanostructures at 300 W, 450 W and 600 W, respectively. Increasing the microwave power has influence on the change in morphology of the as-prepared products [13]. There are a number of nanorods with some irregular shapes were produce at 300 W. Then, Sb_2S_3 nanorods were form, grew and split at 450 W and the prism-like architecture began to form at 600 W. At this stage, the as-obtained product became complete prism-like cluster.

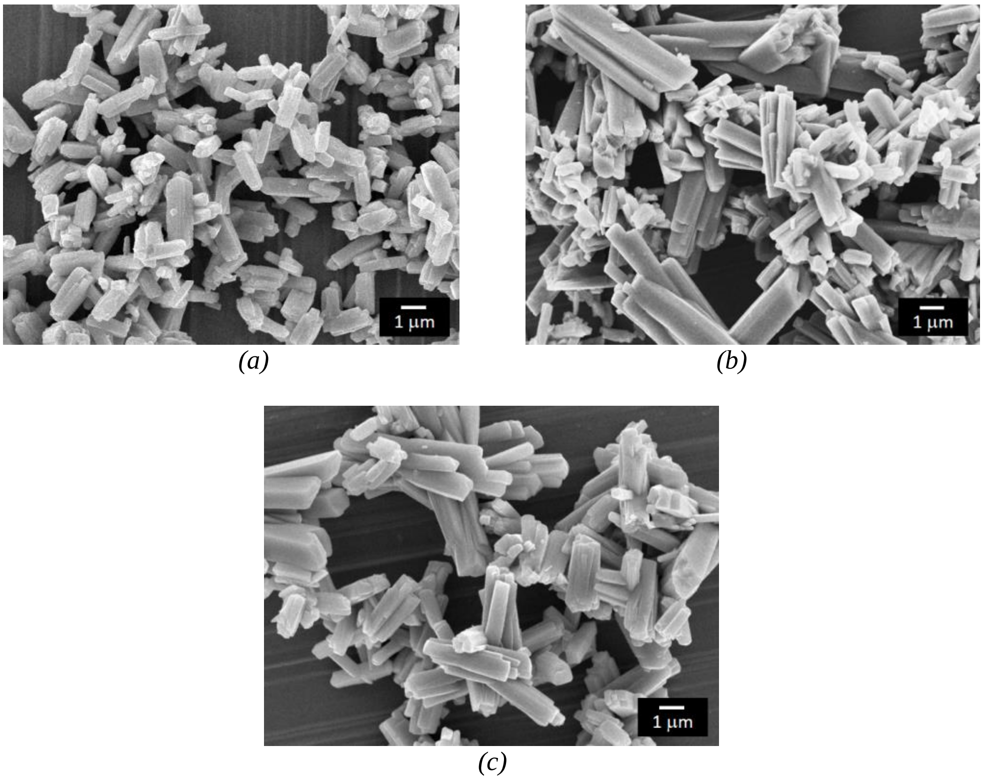

(a) *(b)*

(c)

Fig. 2. SEM images of the as-prepared Sb_2S_3 products synthesized at (a) 300 W (b) 450 W and (c) 600 W for 30 min.

Fig. 3 illustrates the PL spectra of Sb_2S_3 products synthesized at 300 W, 450 W and 600 W, respectively, under excitation at 300 nm. Sb_2S_3 exhibited an emission at 437 nm with some weak shoulders due to the radiant recombination of excitation state electrons [18]. The intensity was increased with the increasing of microwave power, in good accordance with the XRD results [12-13, 19].

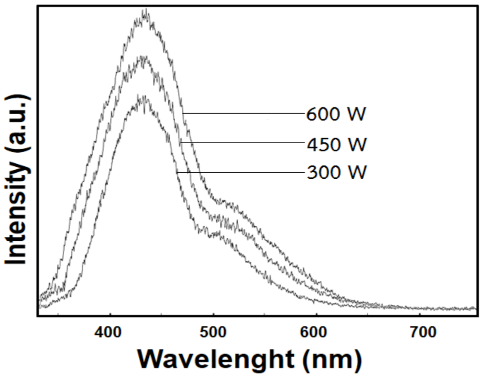

Fig. 3. PL spectra of the as-prepared Sb_2S_3 products .

As can be seen in Fig. 4, EDX spectrum of Sb_2S_3 product at 600 W reveals the element composition of the as-synthesized product. The atomic ratio of Sb:S was 2:3, in good accordance with the stoichiometric composition of Sb_2S_3 chemical formula. No impurities were detected in this spectrum, confirming that the as-synthesized product was pure phase of Sb_2S_3. The peaks at 2.32 keV corresponding to $K_{\alpha1,2}$ line of S, and at 3.61, 3.84, and 4.11 keV corresponding to L_α, $L_{\beta1}$, and $L_{\beta2}$ lines of Sb, corresponding to the previous researches reportet by Zhu *et al.* [5], Abdin *et al.* [7], Yang *et al.* [14], Kavinchan *et al.* [19] and Saksornchai *et al.* [20]. The other peaks were detected that were caused by the electronic transition of copper and carbon tape used for preparing and holding the sample [5, 19].

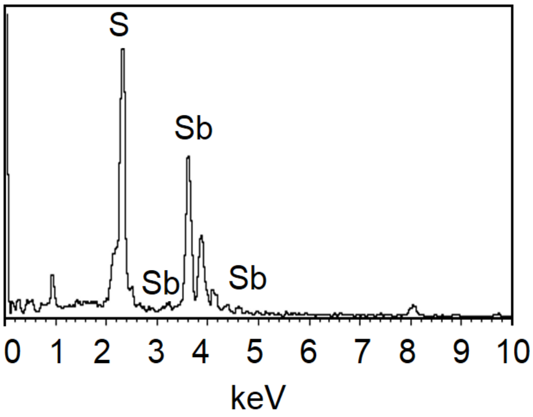

Fig. 4. EDX spectrum of Sb_2S_3 product synthesized at 600 W for 30 min.

Fig. 5 reveals Raman spectrum of Sb_2S_3 product synthesized at 600 W for 30 min. The appearance of the sharp peaks at 148.9 and 190.2 cm^{-1} suggests the formation of crystalline phase of Sb_2S_3 [2, 21-24]. Both of bands at 280.3 and 304.0 cm^{-1} are assigned to the symmetric vibrations of SbS_3 pyramidal units having C_{3v} symmetry – in accordance with the results identified by Boughalmi *et al.* [2], Kärber *et al.* [21], Marquina *et al.* [22], Ota *et al.* [23], and Chalapathi *et al.* [24]. The peak at 252.2 cm^{-1} proved that the as-prepared product is good crystalline as well [25]. It should be noted that the small peak at 450.3 cm^{-1} were also detected – caused by the S-S vibrations or symmetric stretching or Sb-S-S-Sb structural units, corresponding to the previous reports [25-26].

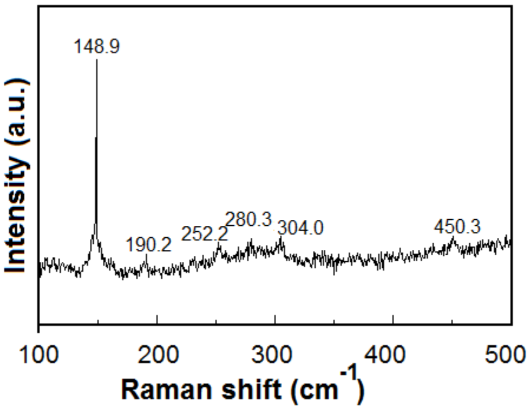

Fig. 5. Raman spectrum of Sb_2S_3 product synthesized at 600 W for 30 min.

In order to study the band structure feature of Sb_2S_3 product synthesized at 600 W. The plots of $(\alpha h\nu)^2$ with respect to hυ of the Sb_2S_3 product is shown in Fig. 6. The direct energy gap of Sb_2S_3 was determined by Tauc plot which can be calculated by this formula:

$$(\alpha h\upsilon)^{1/n} = A(h\upsilon - E_g),$$

where n = 1/2, 2, 3/2, or 3 for the direct-allowed, indirect-allowed, direct-forbidden and indirect-forbidden transition, respectively which n is the adsorption coefficient of the material, h is the Planck's constant, υ is the photon frequency, A is a proportionality constant, and E_g is the optical band gap energy. It can be noted that the band gap energy of Sb_2S_3 is therefore estimated to be 1.50 eV. This band gap energy of as-prepared prism-like Sb_2S_3 product is less than 1.53-1.85 eV of the as-prepared Sb_2S_3 films reported by Abdin *et al.* [7], 1.70 eV of the un-doped Sb_2S_3 film reported by Chalapathi et al. [24] and 2.08 eV of Sb_2S_3 nanorods and 1.80 eV of flowerlike morphology of Sb_2S_3 determined by Ota *et al.* [23]. But, the band gap energy of this research is close to the previous report, for example, the 1.52 eV of Sb_2S_3 nanorods determined by Zhu *et al.* [27], caused by the quantum confinement effect. The decreasing of the band gap energy releated with the increasing of the size of nanostructures [28-29]. In this research, the value of the band gap energy for prism-like Sb_2S_3 is close to the optimum value for photovoltaic conversion, solar energy converters, optical nanodevices and potential solar absorbers or absorbing layers [4].

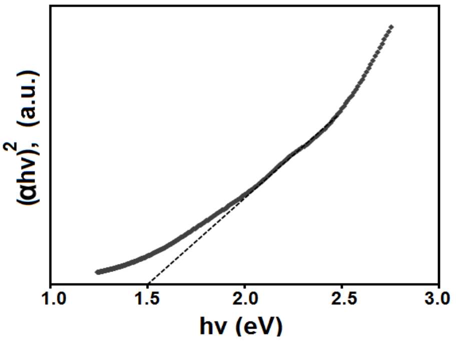

Fig. 6. The plots of $(\alpha h\nu)^2$ and hυ of Sb_2S_3 product synthesized at 600 W for 30 min.

4. Conclusions

In summary, prism-like Sb_2S_3 nanostructures were successfully synthesized by single-step microwave assisted method which is high efficiency process with low cost and green chemistry without using any template. The results also reveal that the as-prepared product was the pure phase of well-crystalline Sb_2S_3 with the optimum band gap energy that can be used as the a prospective material suitable for solar energy conversion, thermoelectric technologies and optoelectronic devices in the IR region.

Acknowledgements

The authors wish to thank School of Science, University of Phayao, Thailand for general support and we are extremely grateful to the Center of Excellence in Materials Science and Technology, Chiang Mai University, Thailand for financial support under the administration of Materials Science Research Center, Faculty of Science, Chiang Mai University, Thailand.

References

[1] Q. Han, Y. Yuan, X. Liu, X. Wu, F. Bei, X. Wang, K. Xu, Langmuir **28**, 6726 (2012).
[2] R. Boughalmi, A. Boukhachem, M. Kahlaoui, H. Maghraoui, M. Amlouk, Materials Science in Semiconductor Processing **26**, 593 (2014).
[3] M. Kriisa, M. Krunks, I. O. Acik, E. Kärber, V. Mikli, Materials Science in Semiconductor Processing **40**, 867 (2015).

[4] M. Kamruzzaman, L. Chaoping, F. Yishu, A. K. Farid Ul Islamc, J. A. Zapien, RSC Advances **6**, 99283 (2016).

[5] J. Zhu, X. Yan, J. Cheng, Nanoscale Research Letters **13**(19), 1 (2018).

[6] Y, Xu, W. Chen, L. Hu, X. Pan, S. Yang, Q. Shen, J. Zhu, Journal of Alloys and Compounds 7**84**, 947 (2019).

[7] Z. U. Abdin, M. H. Alnasir, M. Y. Khan, M. Sajjad, M. T. Qureshi, A. Ullah, A. Zeb, Chalcogenide Letters **16**(1), 37 (2019).

[8] H. Wang,Y. Lu, J. Zhu, H. Chen, Inorganic Chemistry **42**, 6404 (2003).

[9] E. Saksornchai, J. Kavinchan, S. Thongtem, T. Thongtem, Chalcogenide Letters **14**(11), 483 (2017).

[10] J. Kavinchan, T. Thongtem, S. Thongtem, Materials Letters **64**, 2388 (2010).

[11] F. Tian, Z. Wu, Y. Tong, Z. Wu, G. Cravotto, Nanoscale Research Letters **10**(360), 1 (2015).

[12] Powder Diffract. File, JCPDS-ICDD, 12 Campus Boulevard, Newtown Square, PA 19073-3273, USA, (2001).

[13] J. Kavinchan, T. Thongtem, S. Thongtem, E. Saksornchai, Journal of Nanomaterials **2013**, ID719679 (2013).

[14] H. Yang, M. Li, L. Fu, A. Tang, S. Mann, Scientific Reports **3**, 1336 (2013).

[15] S. Srikanth, N. Suriyanaranan, S. Prabahar, V. Balasubramanian, D. Kathirvel, Journal of Optoelectronic and Advanced Materials **12**(10), 2075 (2010).

[16] O. Savado, K.C. Mandal, Solar Energy Materials and Solar Cells **2**, 117 (1992).

[17] K.C. Mandal, A.Mondal, Journal of Physics and Chemistry of Solids **51**, 1339 (1990).

[18] W. Tao, J. Chang, D. Wu, Z. Gao, X. Duan, F. Xu, K. Jiang, Materials Research Bulletin **48**, 538 (2013).

[19] J. Kavinchan, S. Thongtem, E. Saksornchai, T. Thongtem, Chalcogenide Letters **9**(9), 365 (2012).

[20] E. Saksornchai, J. Kavinchan, S. Thongtem, T. Thongtem, Nanoscale Research Letters **12**(589), (2017).

[21] E. Kärber, A. Katerski, I.O. Acik, A. Mere, V. Mikli, Malle Krunks, Beilstein Journal of Nanotechnology **7**, 1662 (2016).

[22] R.G. Marquina, T.G. Sanchez, N.R. Mathews, X. Mathew, Materials Research Bulletin **90**, 285 (2017).

[23] J. Ota, P. Roy, S.K. Srivastava, B.B. Nayak, A.K. Saxena, Crystal Growth & Design **8**(6), 2019 (2008).

[24] U. Chalapathi, B. Poornaprakash, Chang-Hoi Ahn, Si-Hyun Park, Materials Science in Semiconductor Processing **84**, 138 (2018).

[25] C. Pilapong, T. Thongtem, S. Thongtem, Journal of Alloys and Compounds **507**, 38 (2010).

[26] M. A. El Idrissi Raghni, B. Bonnet, M. L. Hafid, J. Olivier-Fourcade, J. C. Jumas, Journal of Alloys and Compounds **260**, 7 (1997).

[27] Q. Zhu, M. Gong, C. Zhang, G. Yong, S. Xiang, Journal of Crystal Growth **311**, 3651 (2009).

[28] S. Kaowphong, T. Thongtem, O. Yayapao, S. Thongtem, Materials Letters **65**, 3405 (2011).

[29] V. N. Soloviev, A. Eichhofer, D. Fenske, U. Banin, Journal of the American Chemical Society **122**, 2673 (2000).